Copyright Warning & Restrictions

The copyright law of the United States (Title 17, United States Code) governs the making of photocopies or other reproductions of copyrighted material.

Under certain conditions specified in the law, libraries and archives are authorized to furnish a photocopy or other reproduction. One of these specified conditions is that the photocopy or reproduction is not to be "used for any purpose other than private study, scholarship, or research." If a, user makes a request for, or later uses, a photocopy or reproduction for purposes in excess of "fair use" that user may be liable for copyright infringement,

This institution reserves the right to refuse to accept a copying order if, in its judgment, fulfillment of the order would involve violation of copyright law.

Please Note: The author retains the copyright while the New Jersey Institute of Technology reserves the right to distribute this thesis or dissertation

Printing note: If you do not wish to print this page, then select "Pages from: first page # to: last page #" on the print dialog screen

NJIT
New Jersey's Science & Technology University

The Van Houten library has removed some of the personal information and all signatures from the approval page and biographical sketches of theses and dissertations in order to protect the identity of NJIT graduates and faculty.

ABSTRACT

DESIGN AND FABRICATION OF A MINIATURE PRESSURE SENSOR HEAD USING DIRECT BONDED ULTRA-THIN SILICON WAFERS

by
Chad Eugene Statler

A miniature pressure sensor head is designed and fabricated using an ultra-thin silicon membrane directly bonded to an excimer laser micromachined substrate. The pressure sensor head has its intended implementation as part of an optically interrogated device with sensitivity to pressures ranging from 0.5 to 4.0 MPa. The pressure range design is shown to be easily adjusted by tailoring the thickness of the membrane wafer. The fabrication process features numerous advantages over existing pressure sensor construction technology including a maskless procedure and no chemical etching or mechanical thinning necessary to form the membrane after bonding. An optic lever is constructed and tested using a reflective aluminum surface. The response of the optic lever device was found to be 160 mV/μm in the linear region.

DESIGN AND FABRICATION OF A MINIATURE PRESSURE SENSOR HEAD USING DIRECT BONDED ULTRA-THIN SILICON WAFERS

by
Chad Eugene Statler

A Thesis
Submitted to the Faculty of New Jersey Institute of Technology and
Rutgers, the State University of New Jersey - Newark Campus
in Partial Fulfillment of the Requirements for the Degree of
Master of Science in Applied Physics

Department of Physics

May 1996

APPROVAL PAGE

DESIGN AND FABRICATION OF A MINIATURE PRESSURE SENSOR HEAD USING DIRECT BONDED ULTRA-THIN SILICON WAFERS

Chad Eugene Statler

Dr. Kenneth R. Farmer, II, Thesis Advisor — Date
Assistant Professor of Physics, NJIT

Dr. John F. Federici, Committee Member — Date
Assistant Professor of Physics, NJIT

Dr. William N. Carr, Committee Member — Date
Professor of Electrical Engineering and Physics, NJIT

BIOGRAPHICAL SKETCH

Author: Chad Eugene Statler

Degree: Master of Science

Date: May 1996

Undergraduate and Graduate Education:

- Master of Science in Applied Physics
  New Jersey Institute of Technology and
  Rutgers, the State University of New Jersey - Newark Campus
  Newark, NJ, 1996

- Bachelor of Arts in Physics
  Shippensburg University, Shippensberg, PA, 1994

Major: Applied Physics

Presentations and Publications:

Chad E. Statler, Elizabeth S. Olson, and K.R. Farmer,
"Design and Fabrication of a Miniature Pressure Sensor Head Using Direct Bonded Ultra-thin Silicon Wafers," *Proceedings of the Ninth Annual International Conference on Microelectromechanical systems Devices (MEMS '96), San Diego, California, USA, February, 1996.*

To my future wife, the lovely Diana

ACKNOWLEDGMENT

I would like to give my deepest appreciation to my advisor, Dr. Kenneth Farmer, for his friendship, guidance, support, and encouragement throughout the past two years. Special thanks to Dr. John Federici and Dr. William Carr for serving as members of the committee. Additional thanks to Dr. Elizabeth Olson and C.H. Wu whose work set the foundation for this project, and to Shawn Washington who measured the infrared transmittance of our ultra-thin silicon wafers.

I would also like to thank Virginia Semiconductor, Inc. of Fredericksburg, Virginia for supplying the ultra-thin silicon wafers and Resonetics, Inc. of Nashua, New Hampshire for performing the excimer laser drilling at a reduced cost.

Portions of this work were completed under grants from the National Science Foundation (ECS-9529616), Virginia Semiconductor, Inc., and the New Jersey Commission on Science and Technology through the Center for Manufacturing Systems.

TABLE OF CONTENTS

Chapter	Page
1 INTRODUCTION	1
1.1 Background and Motivation	1
1.2 Review of the Literature	1
1.3 Overview of the Pressure Sensor	3
2 DESIGN OF THE MINIATURE PRESSURE SENSOR	6
2.1 Design Parameters of Substrate Wafer	6
2.2 Design Parameters of Membrane Wafer	7
2.2.1 Infrared Transmittance of Ultra-Thin Silicon Membrane Wafer	7
2.2.2 Pressure Versus Center Deflection	10
3 FABRICATION OF MINIATURE PRESSURE SENSOR HEAD	14
3.1 Excimer Laser Drilling of Substrate Wafer	14
3.2 Preparation of Membrane Wafer	17
3.3 Direct Bonding of Membrane Wafer	17
3.3.1 Advantages of Direct Bonding Ultra-Thin Silicon	17
3.3.2 Cleanroom Processing	17
3.3.3 Results of Bonding Procedure	20
4 OPTICAL INTERROGATION	22
4.1 Optic Lever	22
4.1.1 Method of Light Detection	22
4.1.2 Advantages of Optical Sensing	24
4.2 Construction of Optic Lever	24
4.3 Evaluation of Optic Lever Performance	26
4.4 Attachment of Fiber Optic to Sensor Head	27
5 CONCLUSION	28

TABLE OF CONTENTS
(continued)

Chapter **Page**

APPENDIX A LIST OF COMPONENTS FOR OPTIC LEVER 30

APPENDIX B IEEE MEMS '96 PAPER 32

REFERENCES 38

LIST OF TABLES

Table **Page**

2.1 Deposition of Si_3N_4 films 9

2.2 Pressure versus center deflection for various membrane materials 11

2.3 Calculated membrane thicknesses for various pressure applications 13

A.1 Components of LED and photodiode circuits 30

A.2 Fiber optic components 31

LIST OF FIGURES

Figure	Page
1.1 Cross section of miniature pressure sensor head	4
2.1 Profile of micromachined substrate wafer	7
2.2 IR transmittance of ultra-thin silicon wafers	8
3.1 Initial hole array of substrate wafer	15
3.2 Transmission IR image of membrane bonded to rough edge	16
3.3 Bonded sensor head structure	20
3.4 Delamination of membrane wafer due to chipout	21
4.1 Optical interrogation scheme	22
4.2 Method of light detection for optic lever	23
4.3 LED circuit	25
4.4 Photodiode circuit	25
4.5 DC photodiode response of optic lever	27

CHAPTER 1

INTRODUCTION

1.1 Background and Motivation

The purpose of this thesis is to present the design and fabrication of a pressure sensor involving the use of new technologies such as excimer laser drilling and direct bonding of ultra-thin silicon wafers. The goal of this project is to present a device with versatility of design, extreme sensitivity to pressures ranging from 4 Pa to 4 MPa, and low manufacturing costs suitable to batch fabrication. The techniques developed here can be extended to many other micro-electro-mechanical systems (MEMS) devices such as controllable micro-mirrors or miniature fluid regulators. Other applications in fields ranging from biophysics to the automotive industry may include "smart" contactless bearings, oil pressure switches and transducers, near-field acoustic holography, artificial touch, and intracochlear measurements of the human ear.

1.2 Review of the Literature

Pressure sensors have been among the first MEMS devices to become commercially successful products. Their success has been due largely to their ease of fabrication and simplicity of design. To date, these sensors have been fabricated using 1) conventional silicon planar processing and sacrificial layers to free active membranes [1] and 2) direct or anodic bonding and the "bond and polish" [2] or "bond and etch" [3] technique to transfer active membranes. In the bond and etch technique for MEMS, an etch-stop layer is formed in a conventional silicon wafer to a depth equal to the desired membrane thickness. After burying this layer by bonding to a micromachined substrate, the unwanted silicon is removed by selective etching, leaving behind membranes over the micromachined features. The main disadvantage of the bond and etch back technique is the small device yield. The bond and polish technique for MEMS offers the same

disadvantage as that of the bond and etch back technique in that polishing after bonding detracts from device yield. This disadvantage is more serious in MEMS applications, where polishing over micromachined structures is a more delicate process than polishing merely over bonded silicon. The bond and etch back technique for MEMS also has disadvantages in that the required doping step adds process complexity. Also, lack of control over doping profile and uniformity leads to variations in membrane uniformity both across individual wafers and from wafer to wafer. Furthermore, the fact that the etch-stop layer must be heavily doped limits electrical applications utilizing the silicon membrane material. All of these disadvantages can be eliminated using ultra-thin silicon membranes directly bonded to micromachined substrates. The membrane thickness is uniform and controllable, no heavily doped etch-stop is required, and any silicon doping concentration may be used. This allows for a wide array of electrical and mechanical applications which use the silicon membrane material to be considered.

In various designs, pressure sensors utilizing piezoelectric, capacitive, and optical sensing have been employed. Pressure sensors utilizing the piezoelectric, or piezoresistive, effect [4]-[8] typically consist of a diaphragm (~ 1 mm in diameter) containing four small strain gauges coupled to form a Wheatstone Bridge. The piezoresistive effect measures the change in resistivity of a material caused by mechanical stress. This effect in silicon is dependent upon the doping concentration of the substrate and the orientation of the crystal. These structures are fabricated by diffusing p-type regions of high electrical conductivity into the n-type diaphragm. Pressure ranges of the resulting transducers vary from 100 kPa to 10 MPa.

Pressure sensors have also been built by micromachining a silicon substrate that is then bonded to a silicon membrane [9]-[13]. The bonded pair acts as the two plates of a simple parallel plate capacitor. As the pressure changes, the silicon membrane is deflected changing the capacitance being measured by a connected resonant LC circuit. These devices are fabricated by etching pits in the substrate with potassium hydroxide

(KOH) and then directly bonding the silicon membrane. The membrane is manually etched back to the desired thickness KOH. The resulting device is typically rectangular in shape with its longest side ~ 2 mm in length. Pressure ranges of the devices are limited to 0 to 40 kPa although they do offer resolution as high as 0.33 percent.

The disadvantages associated with these types of pressure sensors are numerous. Perhaps the greatest drawback to any electrically sensed device (piezoelectric, capacitive, etc.) is its sensitivity to high electromagnetic interference (EMI) environments. In the piezoresistive sensor, the doping of substrate wafers limits future electrical applications. The doping profile may change during diffusion of the strain gauges. The pressure range, although wide, does not offer the high resolution needed for many applications. The capacitive sensor is subject to stray capacitance from the surrounding native oxide layers which could affect measurements and calibration. In addition, both types of sensors require several processing steps such as photolithographical masking and etching which adds to the overall complexity of the device. The relatively large dimensions of these sensors also limits their use in future MEMS applications.

Again, all of these problems can be eliminated by the use of an optics-based sensor formed by the direct bonding of ultra-thin silicon membranes to micromachined substrates. The elimination of EMI sensitivity, the significant decrease in device size, and the reduction in the amount of processing needed to fabricate the device makes our pressure sensor ideal for many applications. A more detailed discussion of pressure sensors employing optical sensing is presented in Chapter 4.

1.3 Overview of Pressure Sensor

We have designed and fabricated a miniature pressure sensor head which is formed using an ultra-thin silicon wafer (~ 5 μm thick) directly bonded to an excimer laser micromachined silicon substrate wafer. The fabrication process features numerous advantages over existing pressure sensor construction technology including a maskless

procedure and no chemical etching or mechanical thinning required to form the silicon membrane. Just four essential steps are needed to build the sensor head: laser micromachining the substrate wafer, fusion bonding the commercially available ultra-thin membrane wafer to the substrate wafer, depositing an IR reflective coating on the outer surface of the membrane wafer, and dicing the individual sensor heads.

Figure 1.1 depicts our miniature pressure sensor head in cross section and illustrates its intended implementation as an optically interrogated device. The sensor head is ~ 200 μm wide and ~ 400 μm thick.

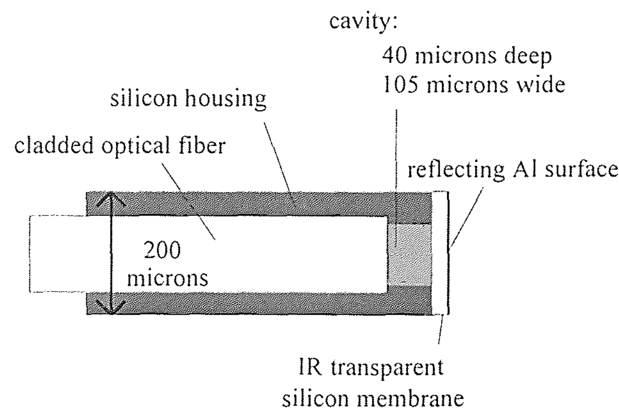

Figure 1.1 Cross section of miniature pressure sensor head.

In the sensor, pressure fluctuations will cause flexing of the ultra-thin silicon membrane that is directly bonded to the surrounding edge of a 105 μm wide, 40 μm deep cavity formed by excimer laser drilling of a standard thickness silicon substrate. Both the membrane and substrate silicon wafers are undoped and therefore transparent to infrared radiation. A 200 nm reflecting layer of aluminum is sputtered onto the membrane's outer surface. This aluminum surface does not affect the deforming properties of the silicon since it accounts for only a small fraction of the total membrane thickness. An optical fiber for sending and receiving IR light is epoxied to the substrate's back surface through

a counterbored socket, with the depth of the counterbore setting the distance between the membrane and the end of the fiber. The membrane's motion is measured through intensity changes in the light that is reflected from the membrane. In this configuration, the sensor operates as an optic lever where variations in the distance between the stationary fiber end and the reflecting membrane cause modulations in the amount of light returning to the fiber. This configuration is simpler than interferometer devices [14] which measure interference-induced light intensity rather than optical deflection induced light intensity variations. The advantages of optical sensing include insensitivity to electromagnetic radiation, use in harsh or toxic environments since the pressure is remotely sensed, and versatility of design both in the geometric shape of the sensor and in the desired pressure range of the device.

CHAPTER 2

DESIGN OF MINIATURE PRESSURE SENSOR HEAD

In the design of our miniature pressure sensor head, we are concerned with several factors: the profile of the micromachined hole in the substrate wafer, the doping (or lack of) concentration of the substrate and membrane wafers, and the thickness of the membrane wafer. In this chapter, we discuss these design parameters for a variety of pressure applications.

2.1 Design Parameters of Substrate Wafer

The substrate wafer used in the design of the miniature pressure sensor head is a standard double-side polished silicon wafer that is readily available. The as-manufactured specifications of this wafer are as follows: 3.990-4.010 inch diameter, $\langle 100 \rangle \pm 0.25°$ orientation, $\geq$1000 ohm-cm resistivity, and 368-395 μm thick. This high resistivity is necessary since the substrate wafer must be transparent to infrared radiation. The stated thickness range is a standard thickness used in the manufacture of silicon wafers. The thickness of the substrate wafer does not affect the performance of the device. The substrate wafer merely serves as the fiber optic holder in our overall design of the pressure sensor head. Figure 2.1 outlines the dimensions of the excimer laser micromachining performed on the substrate wafer.

During fabrication, an ultra-thin silicon membrane is directly bonded to the top side of the 105 μm wide by 40 μm deep cavity. The width of the cavity is smaller than the 125 μm diameter of a standard cladded multimode optical fiber so that the cavity serves as a natural stop for the fiber and sets the baseline depth of the optic lever. The design depth of the cavity is determined by the condition for maximum optic lever sensitivity, namely that the fiber end should be placed roughly one fiber radius away from the reflecting surface [15]. Thus, while our 40 μm deep cavity will allow the use of

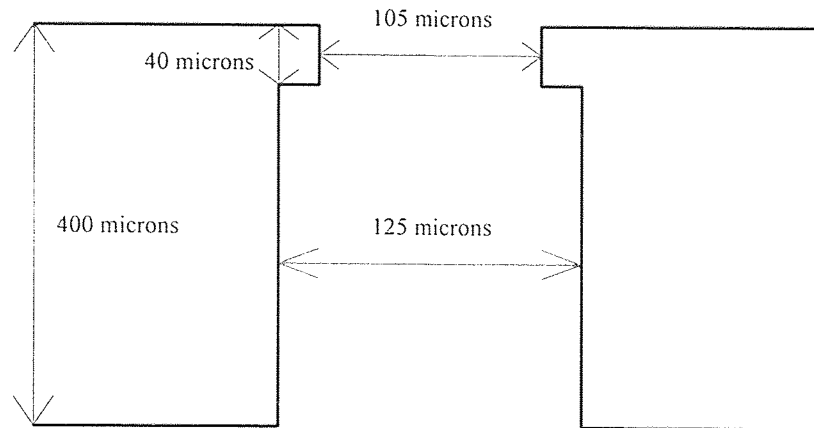

Figure 2.1 Profile of micromachined substrate wafer.

either 50 or 75 μm inner diameter fiber cores, the greater sensitivity is expected for the larger fiber. This condition is verified experimentally in Chapter 4.

2.2 Design Parameters of Membrane Wafer

The membrane wafer used in the design of the miniature pressure sensor head is an ultra-thin, single-side polished silicon wafer [16]. At this time, Virginia Semiconductor, Inc. is the only company known to manufacture ultra-thin silicon wafers. Ultra-thin silicon wafers are commonly designated as those wafers whose thickness is less than 200 μm, which is the limit of conventional silicon polishing technology. The manufactured specifications of the membrane wafer are identical to those of the substrate wafer except for thickness. In our work, the membrane wafers are 5-40.6 μm thick depending on the desired pressure range application. The total thickness variation of the ultra-thin silicon wafer is less than 0.3 μm.

2.2.1 Infrared Transmittance of Ultra-thin Silicon Membrane Wafer

In our design, both the membrane and substrate silicon wafers must be undoped so as to be transparent to infrared radiation. This insures proper calibration of the optic lever. As

infrared light emerges from the optical fiber and bounces off the deposited reflective surface, the corresponding output signal must come directly from the reflective surface and not from the walls of the cavity.

The appropriateness of ultra-thin silicon as an IR transparent material is illustrated in Figure 2.2. Here we have measured the IR transmittance of 5, 10, and 37.5 μm thick wafers for light of wavelength between 800 and 1600 nm.

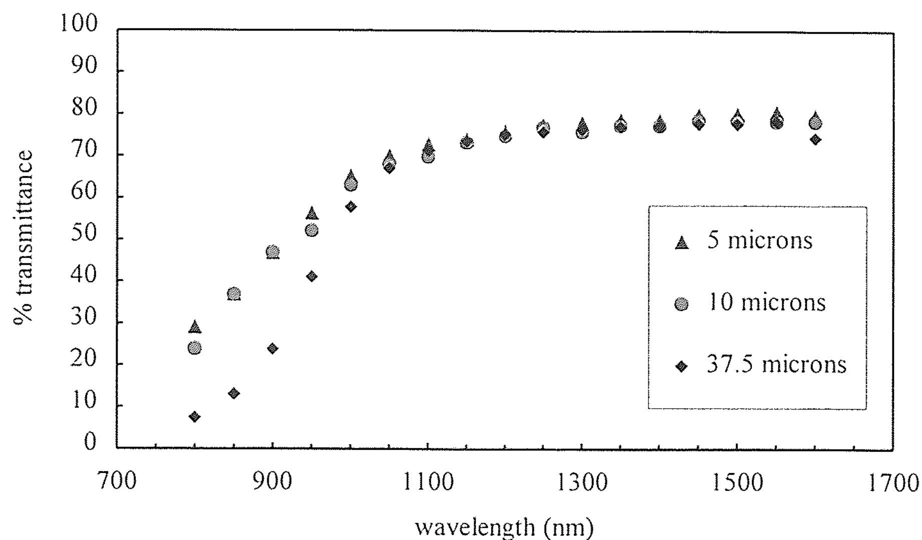

Figure 2.2 IR transmittance of ultra-thin silicon wafers.

All three wafers show approximately the same transmittance in this region of wavelength. These measurements reveal that the same attenuation behavior can be expected of sensor heads made out of any of these thicknesses. So for a given sensor geometry, the device's active pressure range can be tailored by changing the membrane wafer thickness. The following section details this pressure versus center deflection relationship and shows that the device's active pressure range is directly proportional to the thickness of the membrane.

For pressure applications requiring membranes less than 2 μm thick, the membrane material must be changed to either silicon dioxide (SiO_2) or silicon nitride (Si_3N_4) since this is the limit of ultra-thin silicon wafer manufacture. The recipe used for an SiO_2 membrane is the same as that of a wet oxide. This recipe typically calls for an O_2 flow rate of 7.5 SLM with the bubbler set at 530 sccm in a chemical vapor deposition (CVD) furnace for 130 min at 950°C. The SiO_2 is limited to a thickness of ≤ 1 μm because of stress induced on the substrate wafer. These membranes have also proven to be not as robust as deposited Si_3N_4 films.

Silicon nitride membranes can withstand outside stress better than SiO_2 membranes, but they are much harder to bond. However, they can be bonded if a thin oxide is first deposited onto the nitride so that the bonded interface is either SiO_2/SiO_2 or SiO_2/Si. Special consideration must be given to produce stress free Si_3N_4 films using CVD [17]. Table 2.1 summarizes the subtle differences made in the deposition of the two nitride films. Deposition of a stress free Si_3N_4 film is possible for applications which require a membrane thickness of ~ 0.2-2 μm.

Table 2.1 Deposition of Si_3N_4 films.

	Standard Si_3N_4	**Stress free Si_3N_4**
Ambient	1:3 Dichlorosilane:NH_3	5:1 Dichlorosilane:NH_3
Temperature	800°C	840°C

2.2.2 Pressure Versus Center Deflection

The key ingredient in the operation of the pressure sensor device is the thickness of the membrane wafer. This thickness determines the active pressure range of the device and essentially defines its use or application. The ability to tailor the active pressure range of the device is a major advantage to our design. The membrane thickness requirements for any pressure application can be derived from the pressure versus center deflection relationship for a clamped edge circular diaphragm with uniformly distributed load [18].

Deflection at the center of the membrane is given by

$$d = \frac{Pa^4}{64D} \tag{2.1}$$

where P is the load per unit area *i.e.* pressure (dyne cm^{-2}), a is the radius of the membrane (cm), and D is the plate constant (dyne cm).

The plate constant, D, is given by

$$D = \frac{Et^3}{12(1-\nu^2)} \tag{2.2}$$

where t is the membrane thickness (cm), E is the modulus of elasticity for the material (dyne cm^{-2}), and ν is Poisson's ratio for the material.

Substituting Eq. 2.2 directly into Eq. 2.1 and rearranging we get

$$\frac{P}{d} = \frac{64E}{12\left(1-\nu^2\right)}\left(\frac{t^3}{a^4}\right) \tag{2.3}$$

Using the conversion factor 1 Pa = 10 dyne cm^{-2} and the known values of $E = 7.5 \times 10^{11}$ dyne cm^{-2} and $\nu = 0.27$ for silicon [19] we arrive at

$$\frac{P}{d} = \frac{64(7.5 \times 10^{10})}{12[1-(0.27)^2]}\left(\frac{t^3}{a^4}\right) \text{Pa} \tag{2.4}$$

$$\frac{P}{d} = 431 \text{ GPa}\left(\frac{t^3}{a^4}\right) \tag{2.5}$$

The pressure versus center deflection relationship for any material can be derived in exactly the same manner with appropriate values of E and ν [20]-[22] substituted into Eq. 2.3. Table 2.2 summarizes the P versus d relationship for several possible membrane materials. Note the column labeled "C" in Table 2.2 is simply the coefficient of the right hand term in Eq. 2.3 *i.e.*

$$C = \frac{64E}{12\left[1-(\nu)^2\right]} \tag{2.6}$$

Table 2.2 Pressure versus center deflection for various membrane materials.

Material	**E (GPa)**	ν	**C (GPa)**
Si	75	0.27	431
SiO_2	75	0.17	412
Si_3N_4	55-240	0.27	316-1380
Al	70	0.35	425

In all of the pressure versus center deflection derivations made above, P is the ambient pressure relative to the cavity pressure, and d, a, and t are the center deflection, radius, and thickness of the membrane respectively. While these relationships indicate that thinner membranes are more sensitive, the relationships are valid only in a linear approximation of membrane stiffness, *i.e.*, for pressures producing center flexions up to ~ 0.1 times the membrane thickness. For relatively high pressure applications (> 10 Pa), the air gap stiffness can be ignored. Also, the layer of sputtered aluminum can be disregarded in the calculation since it accounts for only a small fraction of the total membrane thickness.

As previously stated, the membrane thickness defines the use or application of the device. For an application requiring an operating pressure range of 0.5 to 4.0 MPa, the design thickness of the membrane can be shown to be ~ 5 μm assuming a diaphragm radius of 52.5 μm.

Using Eq. 2.5 and rearranging for t (assuming $\frac{d}{t} = 0.1$) we get

$$t = \left(\frac{P}{431 \times 10^{8}} \right)^{\frac{1}{4}} a \qquad (2.7)$$

$$t = \left(\frac{4 \times 10^{6}}{431 \times 10^{8}} \right)^{\frac{1}{4}} a \qquad (2.8)$$

$$t \cong 0.1 \text{ a} \qquad (2.9)$$

$$t \cong 5 \ \mu\text{m} \qquad (2.10)$$

The following table summarizes the calculated membrane thicknesses for a variety of pressure applications.

Table 2.3 Calculated membrane thicknesses for various pressure applications.

Diameter (μm)	P_{Max}	P_{Max} **(PSI)**	**Thickness (nm)**
105	4 MPa	582	5100
105	400 kPa	58.2	2900
105	40 kPa	5.82	1600
105	4 kPa	5.82×10^{-1}	900
105	400 Pa	5.82×10^{-2}	500
105	40 Pa	5.82×10^{-3}	300
105	4 Pa	5.82×10^{-4}	160
105	0.4 Pa	5.82×10^{-5}	90

These pressure ranges fall into three major areas of application for our device. Applications in the pressure range above 400 kPa include manufacturing or industrial uses such as a manifold absolute pressure (MAP) sensor for an automobile or a "smart" contactless bearing used by the mining industry. Applications in the 400-40,000 Pa range include *in-situ* monitoring of human body functions and artificial touch. Below the 400 Pa range, applications may include intracochlear measurements and other sensitive research applications.

CHAPTER 3

FABRICATION OF MINIATURE SENSOR HEAD

Fabrication of our miniature pressure sensor head is completed in just four steps: excimer laser drilling of the substrate wafer, direct bonding of the ultra-thin membrane wafer to the micromachined substrate wafer, deposition of a reflective aluminum layer on the top side of the membrane wafer, and dicing the individual sensor heads. In this chapter, the advantages of the excimer laser are discussed in detail. The recipe for our successful ultra-thin bonding procedure is given and supported by infrared photographs of the bonded structure.

3.1 Excimer Laser Drilling of Substrate Wafer

The micromachining of our substrate wafer was performed commercially [23] with an excimer laser. An excimer, or "excited dimer", laser uses a high speed transverse electrical discharge within a mixture of noble and halogen gases during the micromachining process. The average power of an excimer laser is 25-150 W with a typical pulse rate of 50-400 PPS. The wavelength of the laser pulse is 157-351 nm, depending on the laser gas source mixture used, and the energy of the pulse can be as high as 1 Joule. Unlike CO_2 and other "hot" lasers, excimer laser drilling is an ablation technique that does not destroy the crystallinity of the silicon as the drilling takes place. The photo-ablation process can be described as the absorption of deep UV light from the excimer light pulse by the material. The power of the light pulse results in the breaking of the electronic bonds of the material. These fragments form a plasma cloud which carries the thermal energy away from the surface of the material [24]. Little or no damage is produced leaving a surface free of roughness. A clean, smooth surface is a minimum requirement for successful direct bonding of the membrane wafer. The initial hole array of the substrate wafer drilled by the excimer laser is shown in Figure 3.1.

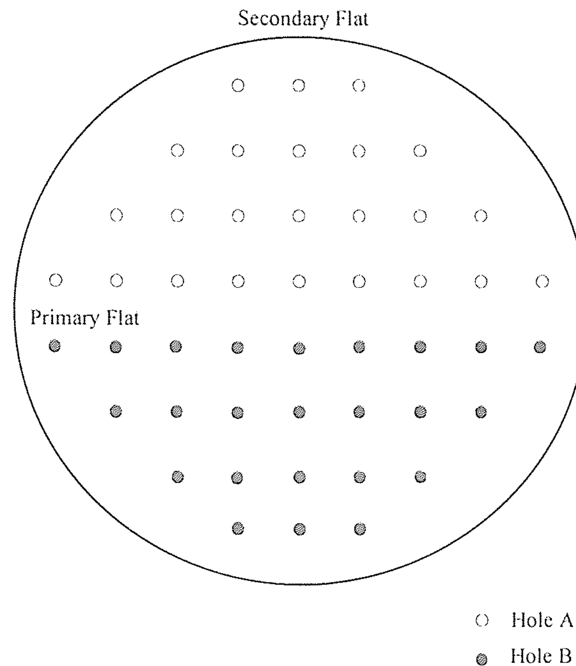

Figure 3.1 Initial hole array of substrate wafer.

Hole A is drilled according to the profile given in Figure 2.1. Hole B is drilled straight through the wafer and is ~ 80 μm in diameter. Both hole profiles are drilled in the following manner: An 80 μm guide hole is drilled from the backside of the wafer according to the hole array give in Figure 3.1. Hole A is widened to 125 μm and countersunk to ~ 40 μm from the top surface of the wafer. The substrate wafer is then turned over and Hole A is widened to 105 μm in diameter. Hole B remains 80 μm in diameter.

This process is noted for the absence of "chipout" on the top side of the substrate wafer for Hole A. However, chipout is present on the top side of the wafer for Hole B. Chipout is the generic term for fragmented material resulting from the drilling process, and is similar to the splintering effect caused by a drill bit on the exit side of a hole drilled through wood. It is critical to the success of the wafer bonding process that the micromachining process not roughen the hole edges, so that bonding occurs completely

to the edge of the cavity. We illustrate this point in Figure 3.2. This figure shows a 100X reflection IR image of a 37.5 μm silicon membrane bonded over part of a 1 cm^2 window opened entirely through a silicon substrate. The image shows the membrane, the rough top and bottom edges of the window formed by a non-excimer laser machining process, and a delamination edge at the bonded interface caused by the roughness. The delamination edge is located tens of microns from the edge of the window.

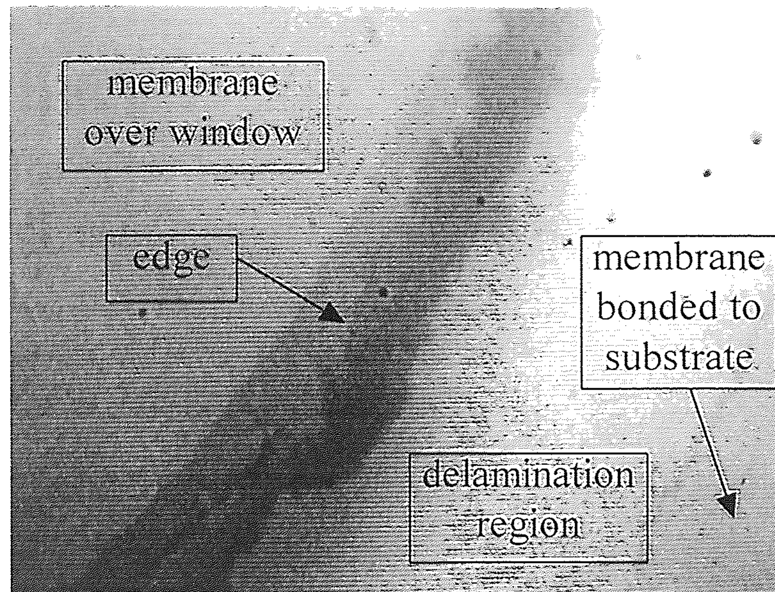

Figure 3.2 Transmission IR image of membrane bonded to rough edge.

We note that often isotropic wet etching is used to form clean edges, but excimer laser ablation offers the advantages of no required masking for photolithograhpic processing. The excimer laser process also produces clean holes with sub-micron positioning accuracy, ~ 3 μm resolution, and cavity walls with roughly 6 degrees of slope. Wet etching leaves a slope that follows the plane of the substrate crystal (~ 54 degrees). We have found that the depth resolution of our 400 μm thick silicon substrate is ~10 μm, but the depth is reproducible from hole to hole on a given wafer.

3.2 Preparation of Membrane Wafer

It is vital to the success of ultra-thin wafer bonding that the surface of the membrane wafer be as clean and smooth as possible. Surface roughness is affected by many factors including: the cleaning process, doping, etching, and the final thinning procedure during manufacture. We have found that polished wafers exhibit greater bondability than those wafers thinned by a final wet etching process during manufacture.

3.3 Direct Bonding

3.3.1 Advantages of Direct Bonding Ultra-Thin Silicon

As stated previously in Chapter 1, direct bonding of ultra-thin silicon membranes to micromachined silicon substrates offers numerous advantages. No masking for photolithographic or wet processing is necessary. No mechanical thinning or chemical etching is needed to form the membrane. The membrane wafer may be doped to any concentration allowing for the use of a wide array of electrical applications. Interface stress due to mismatched thermal coefficients of expansion (TCE) is eliminated by using silicon bonded to silicon. It is commonly known that silicon wafers cannot be polished successfully to thicknesses less than 200 μm using conventional methods. Below this limit, it is difficult to maintain uniformity. In addition, yield decreases significantly due to wafer cracking. Currently, ultra-thin wafers can be produced as thin as 2 μm with a total thickness variation of less than 0.1%. With the need in MEMS for such thin membranes, direct bonding of ultra-thin silicon wafers offers a reasonable approach to device processing.

3.3.2 Cleanroom Processing

Our procedure for bonding ultra-thin silicon generally follows the known procedure for bonding thicker samples [25], but with alterations made in handling, aligning, and

annealing to accommodate the use of ultra-thin silicon. In particular, we find that wafers as thin as 10 μm can be handled mainly in the same manner as conventional wafers since they are self-supporting. However, they cannot be subjected to some of the stresses that ordinary wafers experience such as spin drying. The following bonding procedure for ultra-thin silicon was successfully carried out at the Class 10 cleanroom facility at New Jersey Institute of Technology:

1) Load wafers vertically into adjacent slots of teflon cassette suitable for chemical bathing.

2) "P-Clean" cassette in an aqueous electronic grade solution of 80% H_2SO_4 mixed nominally 5:1 with 30% H_2O_2 10 minutes at 110°C. This clean oxidizes the silicon wafers which enhances the hydrophilic nature of the surfaces and improves bondability [26].

3) Rinse cassette in warm de-ionized water 10 minutes 60-70°C.

4) Rinse cassette in cool de-ionized water 5 minutes 20°C.

5) While preventing contact between the ultra-thin and substrate wafers, carefully blow the wafers dry in a stream of nitrogen gas. Typically, wafers are spun dry in a commercial spin dryer. However, in our case, the ultra-thin wafers cannot survive such rough handling. Note: Complete drying of the wafers is critical to the success of direct bonding. We have found that evaporation of water trapped at the bonded interface can blow the wafers apart during annealing at high temperatures.

6) The wafers are visually aligned along the primary flats by rotating the wafers within their respective slots in the cassette. With care, this action can achieve reasonable crystallographic alignment to ±1°.

7) Room temperature mating occurs by slowly and simultaneously pulling the wafers from their adjacent slots in the cassette. This results in the formation of a "contact wave" along the surface of the joined wafers. Typical contact wave speeds are on the order of 1 cm/sec [27].

8) Visually inspect the wafer pair to insure that there are no obvious voids at the interface. These voids are easily observed as ripples on the thin silicon membrane. Upon annealing, the voids tend to locally rupture the silicon membrane and therefore are to be avoided.

9) Load wafer pair into quartz annealing tube.

10) The wafer pair is pushed into the furnace at a rate of 0.5 mm/sec where the pair sit in a nitrogen ambient flowing at 7.5 L/min at 300°C. We find that heating of the mated stack must occur very slowly, *i.e.*, approximately isothermally, to avoid temperature induced interfacial stress which causes separation of the bonded interface.

11) Once the samples are loaded, the temperature is increased to 1100°C at a rate of 5 deg/min in the same flowing nitrogen environment. At 1100°C, add 2.5 L/min of flowing oxygen to the annealing environment. This anneal is known to strengthen the bond at the interface [28].

12) Anneal for 1 hour at 1100°C.

13) Turn off oxygen flow and ramp furnace temperature down to 300°C at the rate of 5 deg/min.

14) The wafers are pulled from the furnace at 0.5 mm/sec in the flowing nitrogen ambient.

15) Allow wafers to cool and inspect.

Following the bonding procedure, a 200 nm layer of aluminum is sputtered onto the topside of the membrane wafer. This layer acts as the reflective surface in the optical interrogation scheme of our device. Changes in the intensity of the infrared light being carried by the optical fiber will be measured with an optic lever. For the case of a degenerately doped membrane directly bonded to the undoped silicon substrate or using visible light for interrogation, pressure fluctuations can be monitored by reflection from the cavity side rather than the environment side of the membrane.

3.3.3 Results of Bonding Procedure

The results of our successful bonding procedure are shown in the accompanying IR photographs of Figures 3.3 and 3.4. Figure 3.3 shows an IR image, taken from the top side of the membrane, of the bonded sensor head before aluminum deposition. The membrane was bonded to a micromachined hole drilled according to the profile given in Figure 2.1. The photo shows the membrane over the window (center circle), the fiber socket (dark ring), and no evidence of delamination. The hole is approximately 105 μm in diameter. The success of our bonding procedure can be attributed to the absence of chipout on the perimeter of the micromachined hole allowing bonding to occur completely to the edge of the cavity.

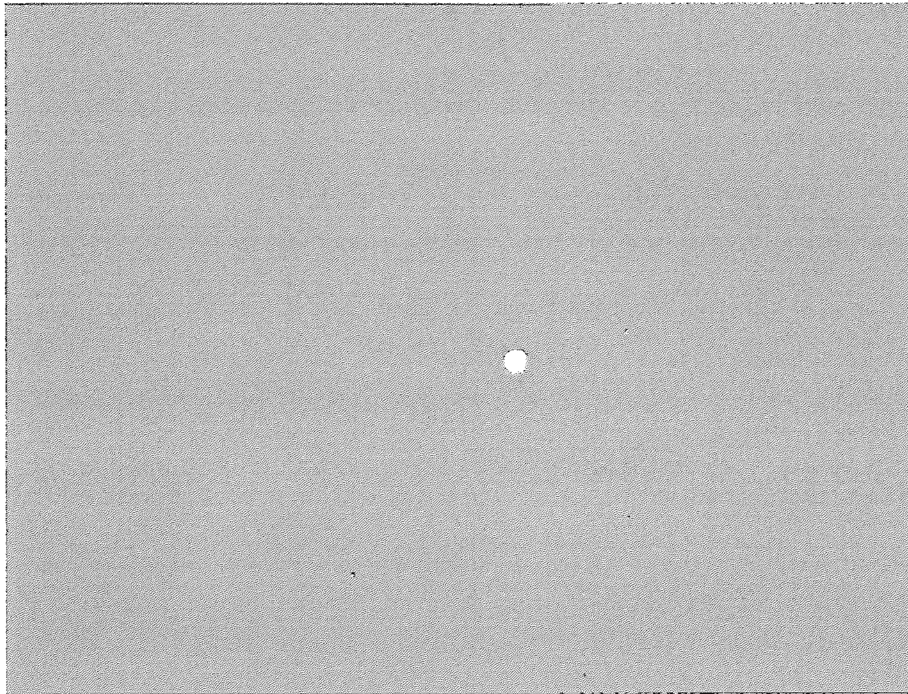

Figure 3.3 Bonded sensor head structure.

Figure 3.4 (using the same field of view as Figure 3.3) illustrates the effect of chipout, or other rough surface structures, on the bonding of ultra-thin silicon wafers. Here the membrane was bonded to a hole drilled according to the description of Hole B found in Figure 3.1. Delamination occurs over a region approximately 2 mm in diameter around the micromachined hole. Again, Figure 3.4 emphasizes the need for clean and smooth surfaces prior to direct bonding of the ultra-thin silicon wafers.

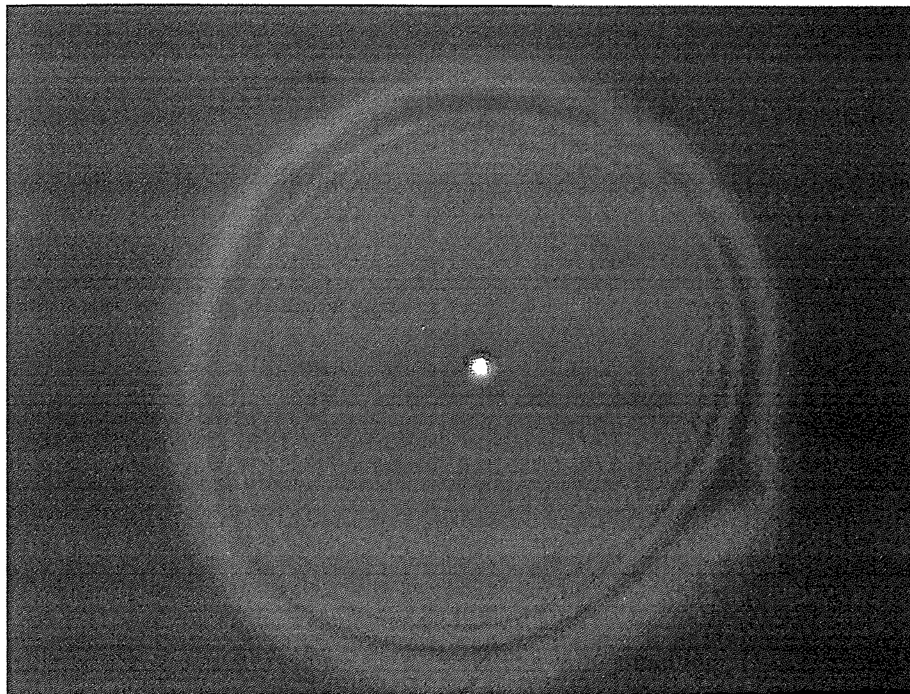

Figure 3.4 Delamination of membrane wafer due to chipout.

Using silicon for both the membrane and substrate material, concern for TCE mismatch at the interface is eliminated. We have cleaved oriented pairs of bonded wafers without separating the thin film from the substrate and observed fracture along one of the crystal planes. This indicates an interfacial bond strength near that of the bulk [29].

CHAPTER 4

OPTICAL INTERROGATION

Our miniature pressure sensor head has its intended implementation as an optically interrogated device. In this chapter, we describe the method of light detection and advantages of an optic lever. We construct an optic lever and evaluate its range of sensitivity. We also discuss the planned attachment of the optical fiber to the miniature pressure sensor head.

4.1 Optic Lever

4.1.1 Method of Light Detection

A fiber optic lever is a position detector. Optic levers have been built in a variety of configurations, but all have been based on the same principle [30]-[34]. Figure 4.1 illustrates the basic principle of an optic lever and shows the intended optical interrogation scheme for our device.

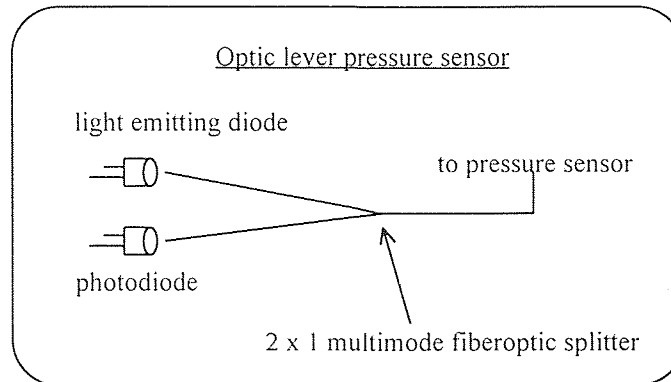

Figure 4.1 Optical interrogation scheme.

In the original configuration of optic lever design, a central fiber is surrounded by a ring of similar diameter fibers forming a fiber bundle. One end of the fiber bundle is positioned close (~ 1 mm away depending upon application) to a reflective surface. At

the other end of the fiber, a broadband light source (typically a light emitting diode) sends light down the middle fiber. Changes in the intensity of light being sent by the central fiber caused by changes in the distance between the fiber end and the reflective surface are measured by this device. At the fiber end, light emerges at all angles (consistent with the numerical aperture of the central fiber [33]) from the central fiber, bounces off the reflective surface, and travels back down the fibers surrounding the central fiber where it is measured by a photodetector. The amount of light that gets back into the fiber ring depends on the distance of the fiber end from the reflective surface. As the reflector moves farther away, the amount of light captured by the fiber bundle decreases accordingly. Figure 4.2 illustrates this concept.

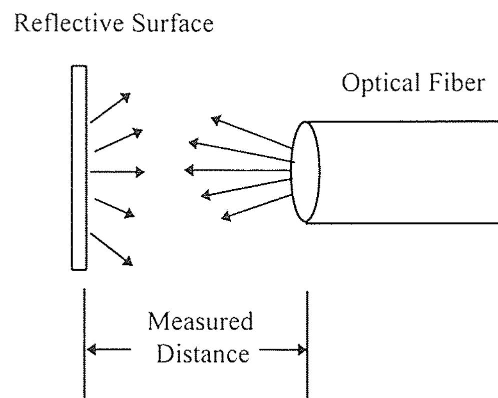

Figure 4.2 Method of light detection for optic lever.

Our optic lever uses only one fiber at the reflector end. It consists of two fibers connected in the middle by a 2×2 multimode fiber optic splitter as shown in Figure 4.1. The two fibers on one side of the splitter are the input (connected to the LED) and the output (connected to the photodiode). The two fibers on the other side are the sensing fiber and an extra fiber that is terminated. The terminated fiber is not shown in Figure 4.1. Light from the LED travels down the fiber and is split 50:50 between the sensing fiber and the terminated end. The sensing end is positioned near the reflecting object

where variations in the distance from the fiber end are measured. In this case, light is reflected back into the same fiber that delivers the light being measured. The returning light is split between the LED and photodiode arms. Only light entering the photodiode arm is measured. This configuration is most useful for measuring small motions. As stated previously in Chapter 2, the sensor is positioned approximately one fiber radius away from the reflective surface for maximum sensitivity.

4.1.2 Advantages of Optical Sensing

The use of optical sensing in the design of this pressure sensor offers numerous advantages. The main advantage to optical sensing is insensitivity to electromagnetic radiation. This sensor can be used in harsh or toxic environments since the pressure is remotely sensed. The design pressure range is easily adjusted by changing the membrane thickness or cavity diameter allowing for a large range of sensitivity to be built into the device. Table 2.3 summarizes the calculated membrane thicknesses for a variety of pressure applications. These pressures range from the sound pressure of the human voice to the high pressures found in manufacturing. Optical sensing allows this pressure sensor to be employed in any of these areas. Other advantages of this design include geometric versatility in the shape of the fiber optic sensor and compatibility with optical fiber telemetry.

4.2 Construction of Optic Lever

The circuits used in the construction of the optic lever device are shown in Figures 4.3 and 4.4. The LED circuit of Figure 4.3 consists of a mounted LED Honeywell™ Model No. HFE4854-014, a 7805 5V voltage regulator, an MPS2222A npn transistor, and a 47 Ω resistor. The LED has a peak wavelength of 850 nm at a maximum current of 80 mA. In our design, the LED must transmit infrared light so that the silicon cavity does not reflect light back into the optical fiber and enhance the output signal of the photodiode

circuit. In order to drive the LED, a 5V voltage regulator is used in series with an npn transistor capable of supplying the necessary 80 mA of current. A 12 V DC power supply is used to power both the 7805 voltage regulator and the LED.

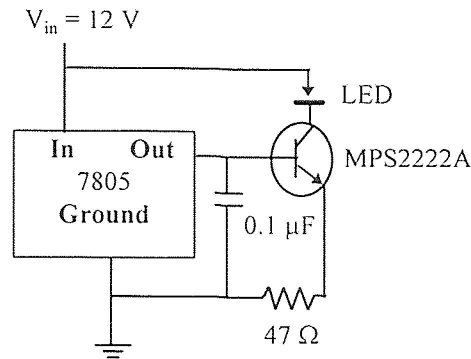

Figure 4.3 LED circuit.

Light reflected back from the surface of the membrane is detected by a photodiode. The photodiode circuit of Figure 4.4 consists of a mounted photodiode Honeywell™ Model No. HFD3874-002, an OP271 op-amp, and various resistors and capacitors. When light hits the photodiode, a current is generated. This current is then converted to an output voltage signal using the op-amp.

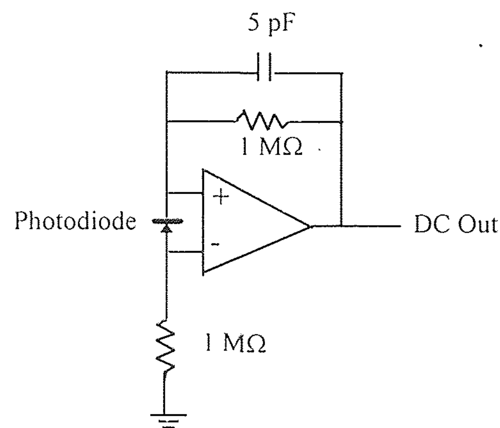

Figure 4.4 Photodiode circuit.

Both circuits are soldered onto a standard PC board and packaged in a generic aluminum box to shield them from outside noise. The cost of the components used in the construction of the optic lever can be found in Appendix A.

4.3 Evaluation of Optic Lever Performance

In Figure 4.5, we evaluate the performance of our optic lever device by measuring the DC response of the photodiode for a reflective aluminum surface using a 50 μm diameter fiber core. To do this, the sensing arm of the lever is mounted to a fiber optic holder and positioned next to a reflective aluminum mirror. The mirror is mounted to a translating stage capable of 1 μm resolution. Output voltage measurements were recorded using a digital voltmeter as the mirror was moved in 5 μm increments. Note this setup is different than the actual optical fiber device described previously. However, it does illustrate the concept of the optic lever where one measures the change in the intensity of the light by varying the distance between the reflective surface and the fiber end. The solid lines of Figure 4.5 indicate the region of useful sensitivity for the device. The maximum slope of the curve in this region is approximately 160 mV/μm. Note that this region is centered on 25 μm. This confirms the general rule of thumb in the design of the cavity depth which states that the region of maximum sensitivity occurs approximately one fiber radius away from the surface.

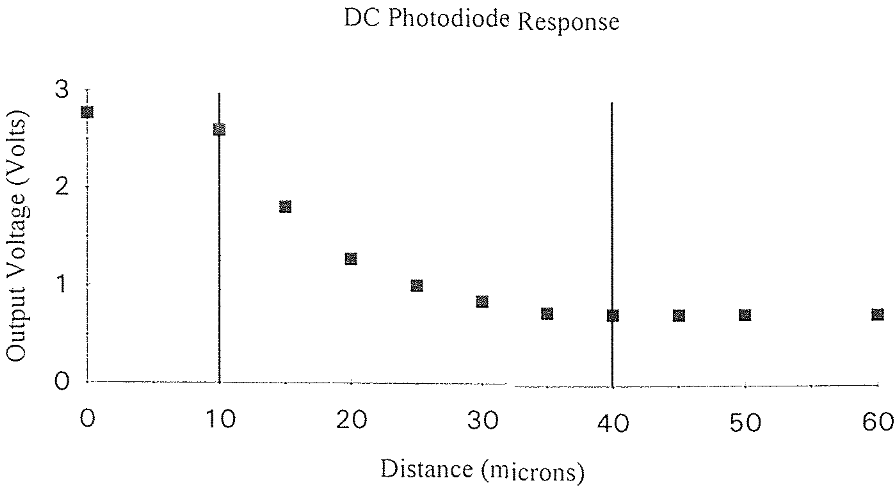

Figure 4.5 DC photodiode response of optic lever.

4.4 Attachment of Fiber Optic to Sensor Head

The final step in the construction of our pressure sensor device is the attachment of the optical fiber to the miniature pressure sensor head. This step has yet to be accomplished. To do this, the individual sensor heads must first be diced (preferably with an excimer laser) and mounted in a 1 mm diameter casing. The optical fiber is then threaded through the backside of the substrate wafer and epoxied. The resulting structure can then be mounted in a standard brass valve cap and connected to a pressure regulator. With the pressure regulator connected to a tank of compressed air, pressure versus center deflection measurements can then be made.

CHAPTER 5

CONCLUSION

We have designed and fabricated a miniature pressure sensor head for use in an optically interrogated device. The sensor head is formed by directly bonding an ultra-thin silicon membrane wafer to an excimer laser micromachined silicon substrate wafer. Direct bonding of the ultra-thin membrane wafer offers the advantage of a maskless procedure with no chemical etching or mechanical thinning necessary to form the membrane after bonding. The pressure range of the device is shown to be easily adjusted by tailoring the thickness of the membrane.

Excimer laser drilling of the substrate wafer offers several advantages in the fabrication process. Excimer laser drilling is an ablation technique that does not distort the crystalline structure of the material as the drilling takes place. This produces a clean, smooth surface which a minimum requirement for successful direct bonding of ultra-thin wafers. The excimer laser process also provides clean holes with sub-micron positioning accuracy, ~ 3 μm resolution, and cavity walls with roughly 6 degrees of slope.

Our miniature pressure sensor head has its intended implementation as an optically interrogated device. For this purpose, we have constructed an optic lever where light transmitted from an LED is carried by an optical fiber to a reflective surface. Changes in the light intensity caused by flexing of the reflective surface are detected by a photodiode. The most useful advantage of optical sensing for a pressure sensor is its insensitivity to EMI radiation. This allows for use in a wide array of electrical and mechanical applications. Other applications to optical sensing include use in harsh or toxic environments since the pressure is remotely sensed and geometric versatility in the shape of the sensor.

Future work on this device includes dicing of the individual sensor heads and attachment of the optical fiber to the backside of the substrate wafer. A possible

improvement to the design of the pressure sensor is the direct bonding of a degenerately doped ultra-thin membrane wafer to the micromachined substrate wafer. This would eliminate the processing step needed to deposit the reflective layer of aluminum on the top side of the membrane wafer. Pressure fluctuations would then be monitored from the environment side of the membrane rather than from the cavity side of the membrane. This improvement is currently under development.

With all of the advantages offered by this device, we expect it to be used in a variety of MEMS applications. Possible applications in the automotive and manufacturing industries include oil pressure switches and transducers, MAP sensors, and "smart" contactless bearings. Biomedical applications include intracochlear measurements of the human ear and *in-situ* monitoring. Other applications for this device include use in the emerging area of near-field acoustic holography as well as controllable micro-mirrors and miniature fluid flow regulators.

APPENDIX A

LIST OF COMPONENTS FOR OPTIC LEVER

In this appendix, we list the part numbers and prices of the components used in the construction of the optic lever. The following components used in the LED and photodiode circuits were ordered from Newark Electronics, Newark, NJ 07102 Catalog #113. Note: These products could possibly be purchased at a local electronics store. The various resistors and capacitors used in the circuit can also be purchased separately at any electronics store.

Table A.1 List of components for LED and photodiode circuits.

Stock #	Item	Price
HFE 4854-014	Mounted LED / Transmitter	$33.07
HFD 3874-002	Mounted Receiver (High Speed)	$25.49
HFD 3854-002	Mounted Receiver	$26.31
MPS2222A	npn Transistor	$ 0.25
MC7805CT	Voltage Regulator	$ 1.12
OP271EZ	High Speed Dual Op-Amp	$10.89

The optical fiber and various connectors were purchased from Gould Electronics (G), Inc., Millersville, MD 21108 and Fiber Instrument Sales (FIS), Oriskany, NY 13424. Table A.2 lists the Model Nos. and prices of the items ordered from these companies.

Table A.2 Fiber optic components.

Model No.	Item	Price
(FIS) 601-IN-SF-50	Fiber Optic Cable 50/125	$ 0.49/meter
(FIS) F1-0010	Fiber Optic Cleaver	$239.00
(FIS) NN203	Fiber Optic Stripper	$ 29.10
(G) 12-0148	Multimode ST Adapter	$ 25.00
(G) 15-31100-50-22121	2×2 Multimode Splitter	$205.00
(G) 64-1132-20-01001	Pigtail Connectors	$ 40.00

APPENDIX B

IEEE MEMS '96 PAPER

The following pages contain a paper presented at the Ninth Annual International Conference on Microelectromechanical Systems Devices (MEMS '96) held in San Diego, California, USA on February 11-15, 1996.

DESIGN AND FABRICATION OF A MINIATURE PRESSURE SENSOR HEAD USING DIRECT BONDED ULTRA-THIN SILICON WAFERS

Chad E. Statler, Elizabeth S. Olson, and K.R. Farmer
New Jersey Institute of Technology
Department of Applied Physics
Newark, New Jersey 07102

Thomas G. Digges, Jr.
Virginia Semiconductor, Inc.
Fredericksburg, Virginia 22401

ABSTRACT

We have designed and fabricated a miniature pressure sensor head which is formed using an ultra-thin silicon wafer (~5 μm thick) directly bonded to an excimer laser micromachined silicon substrate. The fabrication process features numerous advantages over existing pressure sensor construction technology including a maskless procedure and no chemical or mechanical thinning required to form the membrane after bonding. The pressure sensor head forms part of an optically interrogated device with sensitivity to pressures ranging from 0.5 to 4 MPa, but the design pressure range is easily adjusted by changing the membrane thickness or cavity diameter.

INTRODUCTION

Pressure sensors have been among the first micro-electro-mechanical systems (MEMS) to become commercially successful products. Their success has been due largely to their relative ease of fabrication and simplicity of design. To date these sensors have been fabricated using 1) conventional silicon planar processing and sacrificial layers to free active membranes, and 2) direct or anodic bonding and the "bond and polish" or "bond and etch" technique to transfer active membranes. In various designs, piezoelectric, capacitive, electrical and optical sensing have been employed. In the present work we demonstrate that it is possible to further simplify the fabrication of pressure sensors by bonding a silicon membrane directly to a micromachined silicon substrate. Just four essential steps are needed to build the sensor head: laser micromachining the substrate wafer, fusion bonding the commercially available[1] ultra-thin membrane to the substrate, depositing an infra-red (IR) reflective coating, and dicing the individual components. We believe that this is the first report of the use of ultra-thin silicon wafers in the design and fabrication of a pressure sensor. The techniques developed for this project can be extended to many other MEMS devices such as controllable micro-mirrors or miniature fluid flow regulators.

DESIGN

Our miniature pressure sensor head consists of an ultra-thin silicon membrane wafer directly bonded to a micromachined silicon substrate wafer. An optical fiber for sending and receiving IR light is epoxied to the substrate's back surface through a counterbored socket, with the depth of the counterbore setting the distance between the membrane and the end of the fiber. The membrane's motion is measured through intensity changes in the light that is reflected from the membrane. In this configuration, the sensor operates as an optic lever, where variations in the distance between the stationary fiber end and the reflecting membrane cause modulations in the amount of light returning to the fiber. The operational advantages of this design include: 1) a large range of sensitivity (~0.5 to 4 MPa for our design), 2) insensitivity to electromagnetic radiation through the use of optical interrogation, 3) useful in harsh or toxic environments because the pressure is remotely sensed.

0-7803-2985-6/96 $5.00 © 1996 IEEE

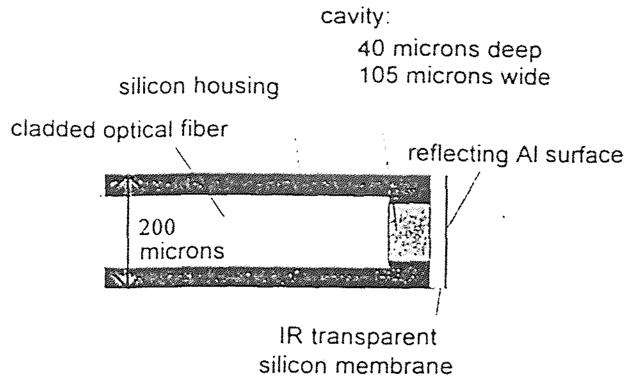

Figure 1. Miniature pressure sensor head.

Figure 1 depicts our miniature sensor head in cross section. The head is ~200 μm wide, in order to accommodate a standard sized (125 μm diameter) optical fiber with cladding, and ~400 μm thick, the combined thickness of the membrane and substrate silicon wafers. The cavity between the membrane and fiber end is 105 μm wide by 40 μm deep. The width of the cavity is smaller than the optical fiber diameter so that the cavity serves as a stop for the fiber, and sets the baseline depth of the optic lever.

Figure 2 illustrates the optical interrogation scheme for our device. Pressure fluctuation induced variations in the distance between the fiber's end and the reflecting membrane cause modulations in the amount of light returning to the fiber and detected by the photodiode. The optically terminated end of the splitter is not shown in the figure.

The design depth of the cavity is determined by the condition for maximum optical lever sensitivity, namely that the fiber end should be placed roughly one fiber radius from the reflecting surface. Thus, while our 40 μm deep cavity will allow the use of either 50 or 75 μm diameter standard multimode fiber cores; the greatest sensitivity is expected for the larger diameter fiber. We have verified this design condition experimentally by measuring the amount of light reflected from a aluminum surface deposited on silicon versus the distance between the fiber end and the reflecting surface. Our results are shown in Figure 3 for a 50 micrometer fiber core. In this case the strongest region of sensitivity falls between the two dashed vertical lines, centered on ~25 micrometers, the radius of the fiber.

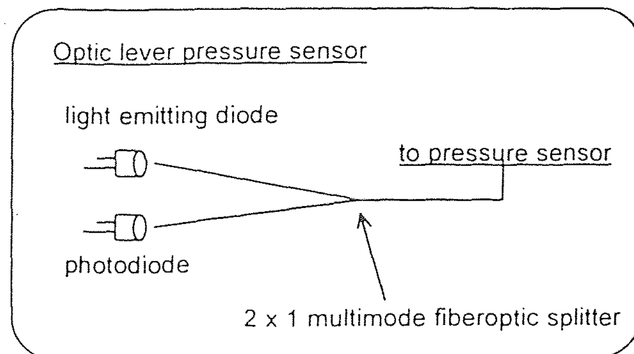

Figure 2. Optical interrogation scheme.

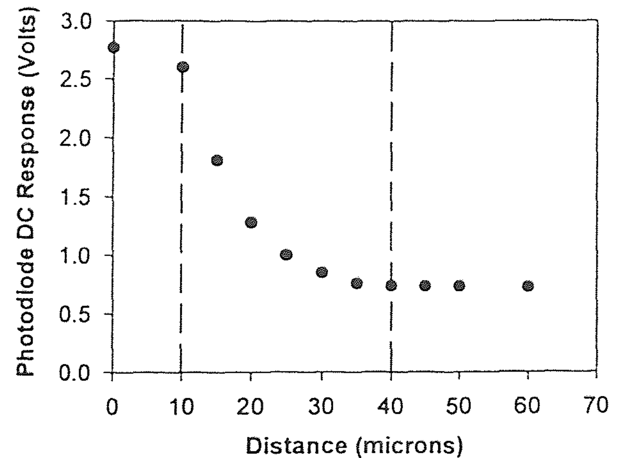

Figure 3. Photodiode response versus optical fiber distance from a reflecting surface. The dashed lines indicate the region of maximum sensitivity.

Both the membrane and substrate silicon wafers are undoped and therefore transparent to infra-red radiation. The appropriateness of the ultra-thin silicon as an IR transparent membrane material is illustrated in Figure 4. Here we have measured the IR transmittance of 5, 10, and 37.5 μm thick wafers for light of wavelength between 800 and 1600 nm. All three wafers show approximately the same transmittance in this region of wavelength. These measurements reveal that approximately the same attenuation behavior can be expected of sensor heads made out of any of these thicknesses. So for a given sensor geometry, the device's active pressure range can be tailored by changing the choice of membrane wafer thickness.

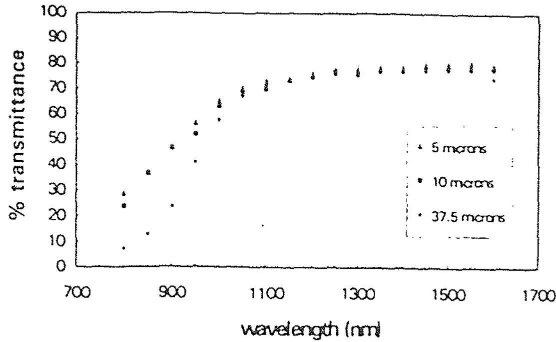

Figure 4. IR transmittance of ultra-thin silicon membranes.

Following direct bonding of the ultra-thin membrane wafer to the substrate wafer, a 200 nm reflecting layer of aluminum is sputtered onto the membrane's outer surface. An alternative to deposition of a reflective layer on the outer surface of the membrane would be the direct bonding of a degenerately doped membrane wafer to the undoped silicon substrate. In this case, pressure fluctuations can be monitored by reflections from the cavity side rather than the environment side of the membrane. This improvement is currently under development.

The membrane thickness required by the high pressure design constraints of our application can be derived from the pressure versus center deflection relationship for a clamped edge circular diaphragm.[2] For a silicon membrane, this relationship is $P/d = 431$ GPa (t^3/a^4), where P is the ambient pressure relative to the cavity pressure, and d, a, and t are the center deflection, radius and thickness of the diaphragm, respectively. While this relationship indicates that thinner membranes are more sensitive, the relationship is valid only in a linear approximation of membrane stiffness, *i.e.*, for pressures producing center flexions up to ~0.1 times the membrane thickness. For high pressure applications, the air gap stiffness can be ignored. Also, the layer of sputtered aluminum can be disregarded in the calculation since it accounts for only a small fraction of the total membrane thickness. For an operating pressure of 4 MPa for maximum linear deflection, and a diaphragm radius of 52.5 µm, the diaphragm design thickness is ~5 µm, within the range of thicknesses tested in Figure 4.

FABRICATION

Four essential steps are needed to fabricate the sensor head: laser micromachining the substrate wafer, fusion bonding the ultra-thin membrane to the substrate, depositing an IR reflective coating, and dicing the individual sensor heads. The first two steps, laser drilling and wafer bonding, have proven to be the most demanding.

For this work, the substrate is a 4", undoped, <100>-oriented silicon wafer, approximately 400 micrometers thick. We used commercial[3] excimer laser drilling to form the sensor cavity and optical fiber socket. This process produces clean holes with ~3 µm resolution, sub-micron positioning accuracy and roughly 6 degree slope. We note that often isotropic wet etching is used to form clean edges, but excimer laser ablation offers the advantages of no required masking for photo-lithographic processing, and near vertical walls of any geometry. We have found that the depth resolution of the counterbore in our 400 µm thick silicon is ~10 µm, but the depth is reproducible from hole to hole on a given wafer. In contrast with CO_2 and other "hot" laser drilling techniques, excimer laser drilling is an ablation technique which does not heat and distort the silicon as the drilling takes place. It is critical for the success of the wafer bonding that the micromachining process not roughen the hole edges, so that bonding occurs completely to the edge of the

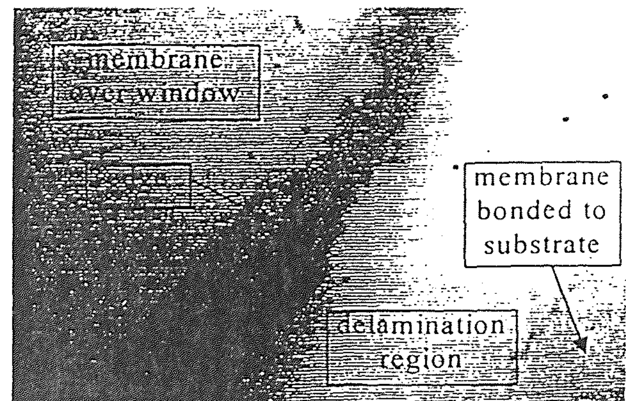

Figure 5. Transmission IR image of membrane bonded over rough edge. Delamination occurs at the bonded interface.

cavity. We illustrate this point in Figure 5. This figure shows a 100X reflection IR image of a 37.5 micrometer silicon membrane bonded over a window opened entirely through a thick silicon substrate. The image shows the membrane, the rough top and bottom edges of the window formed by a non-excimer laser machining process, and a delamination edge at the bonded interface caused by the roughness. The delamination edge is located tens of micrometers from the edge of the window. In contrast, we observe no roughness-induced delamination of thin silicon membranes bonded to our excimer laser drilled holes as long as the bonding is performed on the laser entrance side of the wafer. This is illustrated in Figure 6, an IR image of our completed bonded sensor head structure before aluminum deposition. The photo shows the membrane over the window (center circle), the fiber socket, (dark ring), and no evidence of delamination.

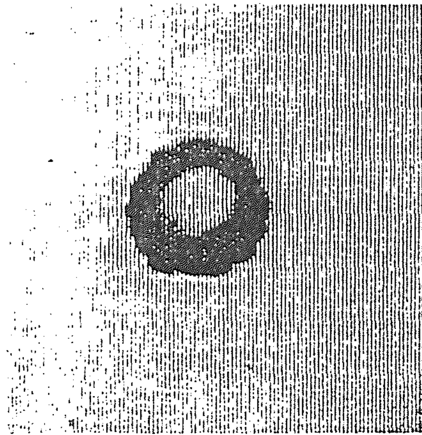

Figure 6. Bonded sensor head structure.

Our procedure for directly bonding the ultra-thin silicon membrane to the micromachined silicon substrate generally follows the known procedure for bonding silicon to silicon[4], but with alterations made in handling, preparation, aligning, and annealing to accommodate the use of ultra-thin silicon. In particular, we find that wafers as thin as ~10 μm can be handled mainly in the same manner as conventional wafers because they are self-supporting. However, they cannot be subjected to some of the stresses that ordinary wafers experience such as spin drying. The ultra-thin wafers must be blown dry gently using N_2 gas. After micro-machining the substrate wafer, we prepare the surfaces of the substrate and membrane wafers by cleaning the wafers in an aqueous, electronic grade solution of 80%-H_2SO_4 mixed nominally 50:1 with 20%-H_2O_2, for 10 minutes at 110 °C. This is the so-called "p-clean." This clean oxidizes the silicon wafers, enhancing the hydrophilic nature of the surfaces, improving bondability. After rinsing in deionized water and drying, the wafers are then mated at room temperature. We have found that leaving the wafers vertical prior to bonding minimizes the chances of trapping airborne particles at the bonding interface. The wafers bond spontaneously once their flats are aligned and a contact wave is initiated by applying slight pressure at the edge of the wafer pair.

A critical step in the successful bonding of ultra-thin wafers is the anneal step which usually follows room temperature mating. We find that heating of the mated stack must occur very slowly, *i.e.*, approximately isothermally, to avoid temperature induced differential interfacial stress which causes separation of the bonded interface. Such stress is not as significant when heating wafers of nominally the same thickness. The details of our successful bonding procedure are listed in Table 1. [5] We have cleaved oriented pairs of wafers bonded using this process, observing fracture approximately along one of the crystal planes, without separating the thin film from the substrate, indicating an interfacial bond strength near that of the bulk.

Table 1. Ultra-thin wafer bonding procedure.

1. P-clean wafers, rinse in deionized water, dry. Resulting surface is hydrophilic, enhancing bondability.
2. Align flats. Join wafers to initiate contact wave.
3. 0.5 mm/sec push into 300 °C annealing furnace. 5 degree/min heat up to 1100 °C.
3. Anneal to increase bond strength: 1100 °C, 1 hr, 3:1 N_2/O_2, 10 l/min flow rate.
4. 5 degree/min cool down to 300 °C.
5. 0.5 mm/sec pull from furnace. Slow push, pull, heating and cooling rates are required for successful bonding.

CONCLUSION

We have described the design and fabrication of a miniature pressure sensor head for use in an optical lever device. The sensor head, which is formed using an ultra-thin silicon wafer (~5 μm thick) directly bonded to an excimer laser micromachined substrate, features a number of distinct advantages over existing pressure sensor technology, both in ease of fabrication and versatility of design. To our knowledge, the successful implementation of such a design, particularly one using ultra-thin silicon wafers as a starting material, has not been presented previously in the literature. We expect that the techniques developed for this project can be extended to many other MEMS devices.

ACKNOWLEDGMENT

Portions of this work were supported by grants from the National Science Foundation (grant number ECS-9529616), the New Jersey Commission on Science and Technology through the Center for Manufacturing Systems, and Virginia Semiconductor, Inc. The authors acknowledge the important contributions of J. F. Federici and Sean Washington for parts of this work. Microfabrication was carried out at NJIT's Microelectronics Research Center.

REFERENCES

[1] Virginia Semiconductor, Inc., Fredericksburg, VA.

[2] S. Way, "Plates", *Handbook of Engineering Mechanics*, Ch. 39, Ed. W. Flugge, McGraw-Hill, 1962.

[3] Resonetics, Inc., Nashua, NH.

[4] See for example: S. Bengtsson and O. Engström, *Journal of the Electrochemical Society*, Vol. 137, p. 2297, 1990.

[5] K. R. Farmer and T. G. Digges, Jr., Patent pending for aspects of ultra-thin wafer bonding.

REFERENCES

[1] E. Arnold, *J. Electrochem. Soc.* **141**, 1983 (1994).

[2] J. Haisma *et al.*, *Jpn. J. Appl. Phys.* **28**, L725 (1989).

[3] W.P. Mazara, *J. Electrochem. Soc.* **138**, 341 (1991).

[4] A.C.M. Gieles and G.H.J. Somers, *Philips Tech. Rev.* **33,** 14-20 (1973).

[5] S.K. Clark and K.D. Wise, *IEEE Trans. Elect. Dev.* **ED-26**, 1887-1896 (1979).

[6] K. Peterson *et al.*, *Proc. IEEE Solid-State Sensor and Actuator Workshop, Hilton Head SC, U.S.A. June 6-9, 1988* pp. 144-147.

[7] W.G. Pfann and R.N. Thurston, *J. Appl. Phys.* **32**, 2008-2019 (1961).

[8] O.N. Tufte and E.L. Stelzer, *J. Appl. Phys.* **34**, 313-319 (1963).

[9] Y. Backlund *et al.*, *Sensors and Actuators* **A21-A23**, 14-20 (1990).

[10] C.S. Sander *et al.*, *IEEE Trans. Elect. Dev.* **ED-27**, 927-930 (1980).

[11] A. Jornod and F. Rudulf, *Sensors and Actuators* **17**, 415-421 (1989).

[12] Y.S. Lee and K.D. Wise, *IEEE Trans. Elect. Dev.* **ED-29**, 42-48 (1982).

[13] C.C. Collins, *IEEE Trans. Biomed. Eng.* **BME-14**, 74-83 (1967).

[14] R.A. Wolthius *et al.*, *IEEE Trans. Biomed. Eng.* **BME-38**, 974-981 (1991).

[15] A. Hu *et al.*, *J. Acoust. Soc. Am.* **91**, 3049-3056 (1992).

[16] Virginia Semiconductor, Inc., Fredericksburg, VA 22401.

[17] Private Communication, K.R. Farmer, (1996).

[18] R.J. Roark, *Formulas for Stress and Strain*, McGraw-Hill, New York, NY (1959).

[19] Ed. W.E. Beadle, *et al.*, *Quick Reference Manual for Silicon Integrated Circuit Technology,* John Wiley and Sons, Inc., New York, NY (1985).

[20] Ed. C. Lynch, *Practical Handbook of Materials Science,* CRC Press, Boca Raton, Florida (1991).

[21] Ed. D. Fink and D. Christiansen, *Electronics Engineers' Handbook,* McGraw-Hill, New York, NY (1992).

[22] Ed. J. Shackelford, *et al.*, *Materials Science and Engineering Handbook,* CRC Press, Boca Raton, Florida (1990).

[23] RESONETICS, Inc., Nashua, NH 03063.

[24] R.D. Schaeffer, *Resonetics Micromachining Seminar Short Course Notes, Princeton, NJ Oct. 17, 1994* pg.17.

[25] S. Bengtsson and O. Engstrom, *J. Electrochem. Soc.* **137**, 229 (1990).

[26] K.Ljundberg *et al.*, *J. Electrochem. Soc.* **141**, 562 (1994).

[27] S. Bengtsson, *J. Elect. Mat.* **21**, 841 (1992).

[28] T. Abe *et al.*, *Ext. Abstr. 22nd Int. Conf. on Solid-State Dev. and Mat.* pg. 853 (1990).

[29] W.P. Maszara *et al.*, *J. Appl. Phys.* **64**, 4943 (1998).

[30] G. He and F. Cuomo, *J. Light. Tech.* **9** 545-551 (1991).

[31] T. Giallorenzi *et al.*, *IEEE J. Quant. Elect.* **QE-16** 626-664 (1982).

[32] F. Cuomo, *J. Acoust. Soc. Am.* **73** 1848-1858 (1983).

[33] R.O. Cook and C.W. Hamm, *Appl. Opt.* **18** 3230-3241 (1979).

[34] G. He and F. Cuomo, *J. Light. Tech.* **9** 1618-1625 (1991).